Preparation and Study of Cu−Al Mixed Oxides via Hydrotalcite-like Precursors

A. Alejandre,[†] F. Medina,[†] P. Salagre,[‡] X. Correig,[§] and J. E. Sueiras*[,†]

Departament d'Enginyeria Química, ETSEQ, and Facultat de Química, Universitat Rovira i Virgili, Pl. Imperial Tarraco 1, 43005 Tarragona, Spain, and Departament d'Enginyeria Electrònica, ETEE, Universitat Rovira i Virgili, Ctra. Salou, s/n, 43006 Tarragona, Spain

Received July 15, 1998. Revised Manuscript Received January 19, 1999

Thermogravimetric analysis (TGA), X-ray diffraction (XRD), BET areas, FT-IR spectroscopy, scanning electron microcopy (SEM) and temperature programmed reduction (TPR) techniques were performed to characterize copper−aluminum mixed-oxide samples with Cu/Al ratios between 0.5 and 3.0. The thermal stability, crystallinity, and purity of the materials obtained depended on the Cu/Al atomic ratio. The FT-IR and TG detected carbonate (mainly) and nitrate as counteranions interacting in the interlayer region. Loosely bound carbonate and nitrate anions and one strongly bound type of carbonate were found. The evolution of phases during calcination was studied using dynamic XRD experiments. The copper hydrotalcite phase is only stable at calcination temperatures lower than 500 K. All the samples showed well-dispersed CuO and/or $CuAl_2O_4$ phases. A pure copper aluminate of high surface area (>150 m^2/g) can be obtained. The rate of formation of copper aluminate depends inversely on the amount of copper in the sample. The TPR experiments showed that all carbonate decomposed at much lower temperatures during the reduction process compared with the decomposition process in a vacuum. However, the consumption of hydrogen was always very close to that required for the stoichiometric reduction of Cu^{2+} to Cu. The degree of reduction of the samples calcined at higher temperatures decreases both with the calcination temperature and the copper content.

Introduction

Hydrotalcites (HT) are a class of layered materials that consist of positively charged brucite $Mg(OH)_2$-like sheets where several Mg^{2+} ions are substituted by trivalent ions such as Al^{3+} and the excess of positive charge is counterbalanced by anions in the interlayer plus water molecules.[1−6]

Anionic clays based on hydrotalcite-like compounds (HT) have many practical applications as catalysts, catalyst supports, ion exchangers, stabilizers, adsorbents, etc. and are among the most investigated catalyst precursors for the remarkable properties of the final catalysts. These include a large surface area, basic properties, high metal dispersion, and stability against sintering, even under extreme conditions.[7−18] Furthermore, all the divalent metals from Mg^{2+} to Mn^{2+} form hydrotalcite-like compounds, with the exception of Cu^{2+}, which forms HT only when other bivalent cations such as Zn, Cr, Co, Mg, Mn, etc. are present.[15−19]

A relatively amorphous CuAl-HT can be prepared by decomposing a copper ammoniacal complex on γ-Al_2O_3.[20] Reichle [21−23] reports the formation of $CuAlCO_3$-HT when the gel obtained by using aqueous solutions of bicarbonate as a precipitant is crystallized at relatively high temperatures.

* Corresponding author. E-mail: jsueiras@etse.urv.es.
† Departament d'Enginyeria Química.
‡ Facultat de Química.
§ Departament d'Enginyeria Electrònica.

(1) Allmann, R.; Lohse, H. H. *N. Jhb. Miner. Mh.* **1966**, *6*, 161.
(2) Allmann, R. *Acta Crystallogr.* **1968**, *B24*, 972.
(3) Ingram, L.; Jepsen, H. P. *N. Jhb. Miner. Mh.* **1967**, *36*, 465.
(4) Taylor, H. F. W. *Miner. Magn.* **1973**, *39*, 377.
(5) Allmann, R. *Chimia* **1970**, *24*, 99.
(6) Cavani, F.; Trifiro, F.; Vaccari, A. *Catal. Today* **1991**, *11*,173.
(7) Trifiro, F.; Vaccari, A. *Comprehensive Supramol. Chem.* **1996**, *7*, 251−292.
(8) Corma, A.; Fornes, V.; Martin-Aranda, R. M.; Rey, F. *J. Catal.* **1992**, *134*, 58.
(9) Corma, A.; Iborra, S.; Prima, J.; Rey., F. *Appl. Catal.* **1994**, *114*, 215.
(10) Climent, M. J.; Corma, A.; Iborra, S.; Prima, J. *J. Catal.* **1995**, *151*, 60.
(11) Tichit, D.; Lhouty, M. H.; Guida, A.; Chiche, B. H.; Figueras, F.; Auroux, A.; Bartalini, B.; Garrone, E. *J. Catal.* **1995**, *151*, 150.
(12) Velu, S.; Swamy, C. S. *Appl. Catal.* **1996**, *145*, 141.
(13) Medina, F.; Tichit, D.; Coq, B.; Vaccari, A.; Dung, N. T. *J. Catal.* **1997**, *167*, 142−152.
(14) Fornasari, G.; Gazzano, M.; Matteuzzi, D.; Trifirò, F.; Vaccari, A. *Appl. Clay Sci.* **1995**, *10*, 69−82.
(15) Gherardi, P.; Ruggeri, O.; Trifirò, F.; Vaccari, A.; Del Piero, G.; Manara, G.; Notari, B. In *Preparation of Catalysts III*; Poncelet, G., Grange, P., Jacobs, P. A., Eds.; Elsevier: Amsterdam, 1983; p 723.
(16) Gusi, S.; Pizzoli, F.; Trifirò, F.; Vaccari, A.; Del Piero, G. In *Preparation of Catalysts IV*; Delmon, B., Grange, P., Jacobs, P. A., Poncelet, G. Eds.; Elsevier: Amsterdam, 1987; p 753.
(17) Doesburg, E. B. M.; Höppener, R. H.; de Koning, B.; Xiaoding, X.; Scholten, J. J. F. In *Preparation of Catalysts IV*; Delmon, B., Grange, P., Jacobs, P. A., Poncelet, G., Eds.; Elsevier: Amsterdam, 1987; p 767.
(18) Busetto, C.; Del Piero, G.; Manara, G.; Trifirò, F.; Vaccari, A. *J. Catal.* **1984**, *85*, 260.
(19) Fornasari, G.; Gusi, S.; Trifirò, F.; Vaccari, A. *Ind. Eng. Chem. Research* **1987**, *26*, 1500.
(20) Herman, R. G., Klier, K.; Simmons, G. W.; Finn, B. P.; Bulko, J. B. *J. Catal.* **1979**, *56*, 407.
(21) Reichle, W. T. *J. Catal.* **1985**, *94*, 547.
(22) Reichle, W. T. *Solid States Ionics* **1986**, *22*, 135.
(23) Reichle, W. T.; Kang, S. Y.; Everhardt, D. S. *J. Catal.* **1986**, *101*, 352.

10.1021/cm980500f CCC: $18.00
Published on Web 03/16/1999

It is also well-known that CuAl-HT is always mixed with other phases such as malachite or gerhardtite due to the Jahn−Teller effect at the Cu^{2+} ion.[21−27]

Yamaoka et al.[24] noticed that $Na_2Al_2(CO_3)_2 \cdot 2.9\ H_2O$ mixed with HT is obtained when Na_2CO_3 is used as a precipitant. Calcination of the latter leads to $NaAlO_2$, which competes with the formation of $CuAl_2O_4$.

On the other hand, supported metal oxide catalysts are widely used in oxidation processes. Mixed oxides crystallizing in the spinel form are potential catalysts for the oxidation of phenol in aqueous solutions.[28] The activity of these catalysts can be related to the BET area of the spinel form.[29] This work aims to synthesize pure copper aluminates with high BET areas using HT as precursors and also to study systematically the nature and characteristics of the CuAl−HT compounds and the chemical changes which take place before the spinel phases are formed.

Experimental Section

Sample Preparation. Four samples of copper−aluminum hydrotalcite-like compounds were synthesized with Cu/Al ratios of 0.5, 1.0, 2.0, and 3.0. They were obtained by coprecipitation from two aqueous solutions at constant pH = 8 ± 0.2. One of them contained appropriate amounts of $Cu(NO_3)_2 \cdot 6H_2O$ and $Al(NO_3)_3 \cdot 9H_2O$ and the other an aqueous solution of triethylamine (1 M). The two solutions were mixed in a glass reaction vessel (volume, 500 cm^3) initially containing deionized water (100 cm^3), where a constant flow of CO_2 was bubbled through the glass reaction vessel, which led to the formation of the carbonate anions in the interlayer region of the solids. The two solutions were added dropwise at room temperature with vigorous magnetic stirring.

The aqueous solution of triethylamine was used as precipitant instead of ammonia or a sodium base to prevent the formation of the copper−ammonia complex and sodium compounds, respectively. The precipitated gels were filtered and washed several times with distilled water. The solids were finally dried in a vacuum at room temperature for 48 h.

The copper−aluminum samples obtained in this way are written as HT*N*(*K*), where *N* is the Cu/Al atomic ratio and *K* the calcination temperature in degrees Kelvin. For example, copper−aluminum hydrotalcite with a Cu/Al atomic ratio of 0.5 will be written as HT0.5 and the corresponding calcined sample at 700 K as HT0.5(700). The calcination process was performed with a heating rate of 1 K/min in air, and the final calcination temperature was maintained for 16 h.

The Cu/Al contents in the coprecipitates were determined by EDAX (energy dispersive analysis using X-ray) and atomic absorption spectroscopy. The results obtained from these techniques are very similar and give the Cu/Al atomic ratios 0.49 (HT0.5), 1.01 (HT1.0), 1.95 (HT2.0), and 2.97 (HT3.0), which agree with the expected values.

Although a flow of CO_2 was bubbling through the solution during the synthesis of the materials, the coprecipitates contain both nitrate and carbonate as charge-compensating anions (see Table 1). This could be explained by taking into account the pH of precipitation (=8), the capability of CO_2 to form carbonate species under these pH conditions, and the similar size of both anions. The *c* parameter of the copper hydrotalcite-like materials has been calculated from the (003) reflection, and the structural formulas were established from the chemical analysis of the solids, the thermogravimetric data, and the mass spectra (see Table 1).

Table 1. Compositions of the Samples and *c* Parameters

sample	composition	*c* (Å)
HT0.5	$Cu_{0.33}Al_{0.67}(OH)_{2.283}(NO_3)_{0.067}(CO_3)_{0.161} \cdot 1.88H_2O$	23.065
HT1.0	$Cu_{0.50}Al_{0.50}(OH)_{2.14}(NO_3)_{0.05}(CO_3)_{0.154} \cdot 1.29H_2O$	22.982
HT2.0	$Cu_{0.66}Al_{0.34}(OH)_{1.966}(NO_3)_{0.027}(CO_3)_{0.173} \cdot 0.78H_2O$	22.848
HT3.0	$Cu_{0.748}Al_{0.252}(OH)_{2.02}(NO_3)_{0.01}(CO_3)_{0.11} \cdot 0.58H_2O$	22.856

BET Areas. BET surface areas were calculated from the nitrogen adsorption isotherms at 77 K by using a Micromeritics ASAP 2000 surface analyzer, and a value of 0.164 nm^2 for the cross section of the nitrogen molecule. The same equipment automatically calculates the pore distribution by the Barret, Joyner, and Halenda (BJH) method.[30]

X-ray Diffraction (XRD). Powder X-ray diffraction (XRD) patterns of the catalysts were obtained with a Siemens D5000 diffractometer by using the nickel-filtered Cu Kα radiation. The structural evolution during thermal treatment in air was monitored in situ with a high-temperature XRD attachment. These thermal treatments were performed under flowing air (100 mL/min) from room-temperature rising to 1273 K with conditions of sequential temperature increase (2 K/min) and of temperature holding time (1 h) before each measurement. The patterns were recorded over a range of 2θ angles from 5° to 85° and compared to the X-ray powder references to confirm phase identities. The patterns of the detected phases are $Cu_2(OH)_3NO_3$ gerhardtite (JCPDS-ICDD 14-687), $Cu_2(CO_3)(OH)_2$ malachite (JCPDS-ICDD 41-1390), $Cu_6Al_2(OH)_{16}\ CO_3 \cdot 4H_2O$ (JCPDS-ICDD 37-630)], CuO tenorite (JCPDS-ICDD 41-254), $CuAl_2O_4$ (JCPDS-ICDD 33-448), and $Al(OH)_3$ gibbsite (JCPDS-ICDD 7-0324).

FT-IR Spectroscopy. The FT-IR spectra were recorded on a Nicolet 5ZDX spectrometer in the 4000−400 cm^{-1} wavenumber range using pressed KBr pellets. The quartz cell with KBr windows was connected to a vacuum line (10^{-3}−10^{-6} Torr) for thermal treatment in a controlled atmosphere.

Thermal Analysis. The thermogravimetric analyses (TG) were carried out on a Perkin-Elmer TGA 7 microbalance with an accuracy of 1 μg and equipped with a 272−1273 K programmable temperature furnace. Samples of 25 mg were heated at 5 K/min up to 1173 K in a flow of dry helium (80 mL/min). The nature of the gases that evolved during the thermal decomposition process was monitored with a QTMD FISONS mass spectrometer.

Temperature Programmed Reduction (TPR). This technique was carried out on a Perkin-Elmer TGA 7 microbalance with an accuracy of 1 μg and equipped with a 273−1273 K programmable temperature furnace. Samples of 25 mg were heated at 25 K/min from room temperature to 1173 K in a flow of a dry H_2/Ar mixture (H_2/Ar, 5/95 vol). The nature of the gases that evolved and the hydrogen consumption during the TPR experiments were monitored with a FISONS MD 800 mass detector.

Scanning Electron Microscopy (SEM). The scanning electron micrographs were obtained with a JEOL JSM-6400 microscope operating at acceleration voltages = 30−35 kV, working distances = 8−19 mm, and magnification values up to 100.000×.

Results and Discussion

BET Areas. Table 2 shows the results of the BET and porosimetry determinations that include the BET surface areas and the average pore diameters (Å) for the samples calcined at different temperatures between

(24) Yamaoka, T.; Abe, M.; Tsuji, M. *Mater. Res. Bull.* **1989**, *24*, 1183.
(25) Trifirò, F.; Vaccari, A.; Del Piero, G. *Stud. Surf. Sci. Catal.* **1988**, *39*, 571.
(26) Kannan, S.; Swamy, C. S. *Appl. Catal. B* **1994**, *3*, 205.
(27) Köckerling, M.; Geismar, G.; Henkel, G.; Nolting, H. F. *J. Chem. Soc., Faraday Trans.* **1997**, *93*, 481−484.
(28) Alejandre, A.; Medina, F.; Fabregat, A.; Salagre, P.; Sueiras, J. E. 3rd World Congress of Oxidation Catalysis; San Diego, CA, proceeding abtracts K-2, September 1997.
(29) Alejandre, A.; Medina, F.; Fabregat, A.; Salagre, P.; Sueiras, J. E. *Appl. Catal. B: Environ.* In press).
(30) Barrett, E. P.; Joyner, L. G.; Halenda, P. P. *J. Am. Chem. Soc.* **1951**, *73*, 373.

Table 2. Specific Surface Area and Average Pore Diameter (APD) for the Samples Calcined at Different Temperatures

	HT0.5		HT1.0		HT2.0		HT3.0	
calcination temp (K)	BET area (m^2/g)	APD (Å)	BET area (m^2/g)	APD (Å)	BET area (m^2/g)	APD (Å)	BET area (m^2/g)	APD (Å)
393	181	127	97	155	77	137	47	117
473	161	117	108	135	74	127	64	98
673	217	138	98	156	70	158	57	118
873	190	153	92	169	65	159	57	117
923	150	170	83	175	60	166	53	110
1073	53	247	22	177	35	133	22	102
1273	2		2		2		2	

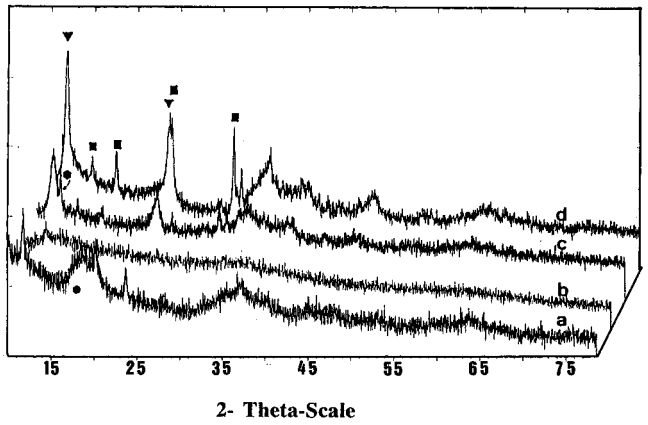

Figure 1. X-ray diffractograms of noncalcined HT0.5 (**a**), HT1.0 (**b**), HT2.0 (**c**) and HT3.0 (**d**) samples. Symbols indicate the presence of copper hydrotalcite (▼), malachite (■), gerhadtite (⬢) and gibbsite phases (●).

393 and 1273 K. The composition of the sample and the calcination temperatures have a strong influence on the surface areas. When both the copper concentration of the sample and the calcination temperatures increase, the BET area values decrease.

The surface areas are usually highest for the samples calcined between 393 and 873 K, which corresponds with the disappearance of the HT XRD pattern[14] (see below in XRD). The BET area decreases considerably when the samples are calcined at 1273 K (at the formation of the spinel phase). Sample HT0.5 has always the highest surface area at any calcination temperature. This can be attributed to the formation of more amorphous phases such as hydroxides−carbonates and alumina hydrate phase (gibbsite) instead of the hydrotalcite phase during the coprecipitation process, probably due to their lower divalent/trivalent ratio.[6] This gibbsite phase was also poorly crystallized and barely detected by XRD. The increase in surface area at relatively low temperatures may be related to the desorption of water and CO_2.[23] All the samples show average pore-diameter values in the range 100−250 Å. When the calcination temperatures are lower than 1000 K, the solids show a mesoporous texture, in contrast to the absence of porosity when the solids are calcined at 1273 K. The samples calcined at lower temperatures also exhibit type IV isotherms according to the classification of Brunauer, Deming, Deming, and Teller (BDDT).[31]

X-ray Diffraction (XRD). Figure 1 shows the X-ray powder patterns of the samples at room temperature, while Table 1 shows the *c* parameters. A sligth increase in this parameter is detected for the HT0.5 and HT1.0 samples, probably due to the higher amount of nitrates as compensating anions.[6,7] The following phases were detected: for the sample HT0.5, copper hydrotalcite, malachite, and gibbsite (all these phases had poor crystallinity); for HT1.0, copper hydrotalcite phase; for HT2.0, copper hydrotalcite, malachite, and gerhardtite; and for HT3.0, copper hydrotalcite and traces of malachite. Figure 1 shows that essentially amorphous materials are obtained mainly from HT0.5 and HT1.0 samples. Yields of copper hydrotalcite phase are higher when the copper content of the sample increases; this agrees with the data reported in the literature that a divalent/trivalent molar ratio equal or larger than 2.0 is needed to prepare crystallographically pure hydrotalcites.[6]

To see just how much XRD order these materials have, a mixture of each one was analyzed (with different amounts of Si) by XRD using the method of Rietveld.[32] The yield of the hydrotalcite phase was 10, 25, 55, and 85% for HT0.5, HT1.0, HT2.0, and HT3.0, respectively. Consequently, the majority of the products obtained from HT0.5 and HT1.0 samples were amorphous hydroxides−carbonates (probably also amorphous hydrotalcite-like phases).

To obtain greater cristallinity, a hydrothermal treatment (bubbling CO_2) was performed at 333 K for 48 h.[33−35] All the samples then showed an increase in malachite and gibbsite phases, which destroyed the copper hydrotalcite phase either partially (for HT2.0 and HT3.0) or totally (for HT0.5 and HT1.0). This agrees with the data reported in the literature.[18] If the hydrothermal treatment is performed without CO_2, well-crystallized gerhardtite and gibbsite phases are only detected for the HT0.5 and HT1.0 samples, and the copper hydrotalcite phase for the HT2.0 and HT3.0 samples is partially destroyed. Then, to obtain more copper hydrotalcite phase, aging processes that improve the more stable phases such as malachite and gerhardtite must be avoided. This opposite behavior compared with other hydrotalcite-like compounds can be attributed to the lower stability of the copper hydrotalcite phase due to the Jahn−Teller effect in the Cu^{2+} ion.

Recent reports describe the formation of thermally metastable phases from Mg/Al layered double hydroxide by performing in situ high-temperature powder X-ray

(31) Brunauer, S.; Deming, L. S.; Deming, W. S.; Teller, E. *J. Am. Chem. Soc.* **1940**, *62*, 1723.

(32) Rietveld, H. A. *J. Apll. Cryst.* **1969**, *2*, 65.

(33) Roy, A.; Forano, C.; Malki, D.; Besse, J. In *Synthesis of Microporous Materials, V. II, Expanded Clays and Other Microporous Solids*, Occelli, M. L., Robson, H. E., Eds.; Van Nostrand Reinhold: 1992; pp 108−169.

(34) Bish, D. L.; Brindley, G. W. *Am. Miner.* **1977**, 62, 458.

(35) Hernandez- Moreno, M. J. H.; Ulibarri, M. A.; Rendon, J. L.; Serna, J. L. *Phys. Chem. Miner.* **1985**, *12*, 34.

diffraction (HTXRD) during the calcination process.[36] These metastable phases are sometimes missed in conventional XRD measurements since measurements are made after the samples have been heated and cooled away from the XRD sample chamber.

So to detect the appearance of some metastable phase and also study the transition of copper oxide to copper aluminate phase more accurately, several experiments were performed using a high-temperature chamber (HTK Anton Paar) attached to the X-ray diffractometer.

The change in the X-ray diffraction pattern on heating from 333 to 1273 K is shown in Figure 2 and Table 3.

Figure 2 shows the diffraction lines of copper aluminum oxide (JCPDS-ICDD 33-0448) given as a reference. Metastable phases from copper hydrotalcite have not been detected, in contrast with the data reported from Mg/Al hydrotalcite phase.[36]

Heating at temperatures higher than 473 K causes the decomposition of all the phases detected by XRD (copper hydrotalcite, malachite, and gerhardtite phases).

However, Mg/Al/CO_3 hydrotalcite phase is stable at temperatures greater than 650 K.[6] The lower stability of the copper hydrotalcite-like phase is probably responsible for the lack of some metastable phase. It should be pointed out that the malachite phase is stable at 473 K only for the sample HT2.0.

The calcination of samples HT0.5 through HT3.0 between 473 and 673 K yields an incipient CuO phase, with the smallest crystals at a lower Cu/Al ratio. An incipient tenorite phase (CuO) is detected for the sample HT0.5 (which has the lowest Cu/Al atomic ratio) at calcination temperatures between 473 and 873 K. Moreover, a well-crystallized copper aluminate phase is also detected at 1073 K.

On the other hand, samples HT2.0 and HT3.0, which have the highest Cu/Al atomic ratios, show a well-crystallized CuO phase at 673 K. The intensities of the characteristic CuO diffraction lines increase between 473 and 873 K, with the increase in copper content. This CuO phase appears together with the copper aluminate phase at higher calcination temperatures (>923 K).

Furthermore, for sample HT0.5, which has the same Cu/Al atomic ratio as the stoichiometric copper aluminate, the amorphous CuO phase turns into a well-crystallized and nearly pure copper aluminate at lower calcination temperatures (<923 K).

The CuO and $CuAl_2O_4$ crystallite sizes (calculated from the Sherrer equation) of the samples calcined at different temperatures are summarized in Table 3. CuO and $CuAl_2O_4$ particles were between 3.5 and 55, and 6 and 53 nm, respectively, at the different calcination temperatures tested. Table 3 shows that particles of CuO and $CuAl_2O_4$ are larger when both the Cu/Al atomic ratio and the calcination temperature increase.

The structural evolution around the transition temperature of the CuO to $CuAl_2O_4$ is shown in Figure 3.

From this figure, we can see that the copper aluminate begins to form at a temperature around 973 K for sample HT0.5, which agrees with the literature,[37,38] while for sample HT3.0, which has the highest copper content, it begins to form at about 1223 K. Furthermore, it should be noted that all the samples calcined at 950 K for 24 h showed the formation of a stoichiometric copper aluminate phase.

The rate of formation of copper aluminate is therefore strongly lowered by high contents of copper in the sample. This could be explained by the formation of

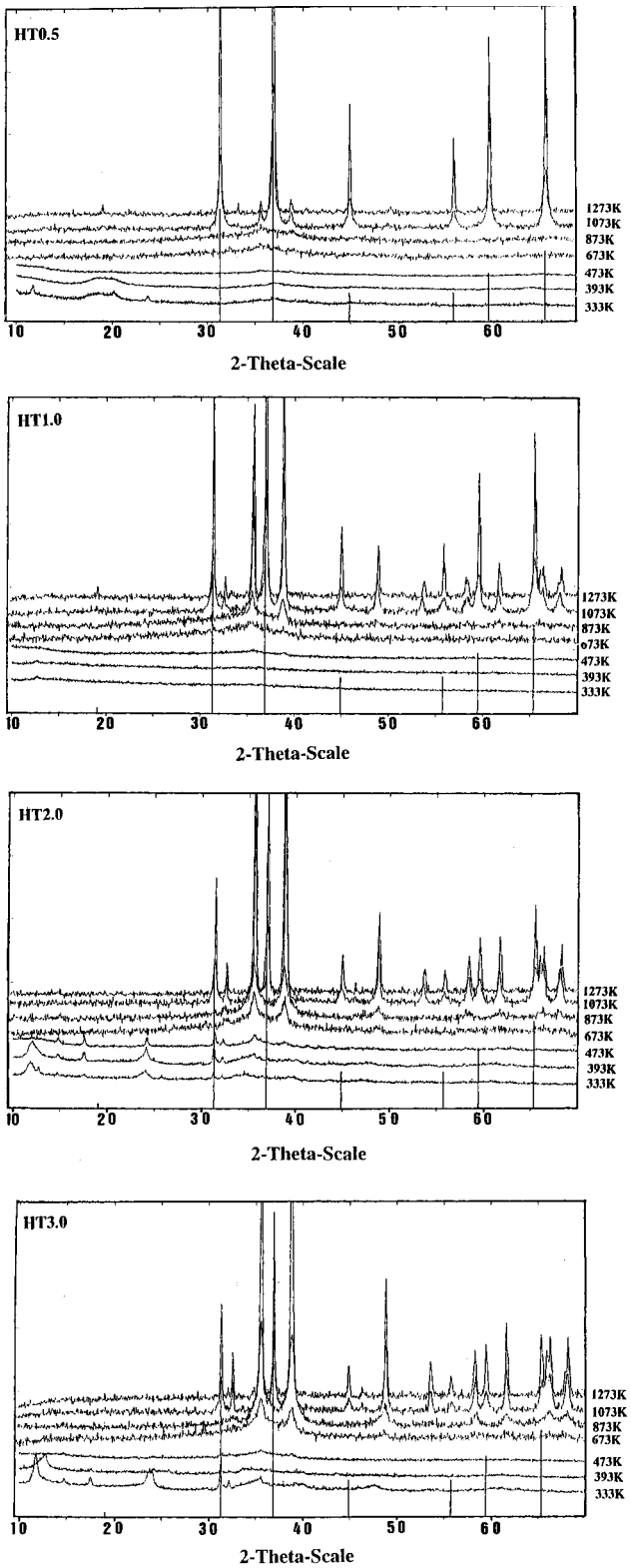

Figure 2. Evolution of the X-ray diffractograms versus calcination temperatures between 333 and 1273 K of the (a) HT0.5, (b) HT1.0, (c) HT2.0, and (d) HT3.0 samples. The diffraction lines of copper aluminum oxide are also showed.

(36) Kanezaki, E. *Inorg. Chem.* **1998**, *37*, 2588.
(37) Jacob, K. T.; Alcock, C. B. *J. Am. Ceram. Soc.* **1975**, *38* (5−6), 192−195.
(38) Susnitzky, D. W.; Carter, C. B. *J. Mater. Res.* **1991**, *6*, 1958.

Table 3. Crystallite Sizes (Å) and Phases Detected by XRD for the Samples Calcined at Different Temperatures[a]

calcin temp (K)	HT0.5	HT1.0	HT2.0	HT3.0
333	HT Ma Gi	HT	HT(154) Ma Ge	HT(169) Ma
393	HT Ma Gi	−	HT(98) Ma Ge	HT(101) Ma
473	−	CuO(46)	CuO(89) Ma	CuO(80) Ma
673	CuO(35)	CuO(57)	CuO(128)	CuO(120)
873	CuO(45)	CuO(190)	CuO(203)	CuO(198)
923	CuO(60) $CuAl_2O_4$(60)	CuO(220)	CuO(280)	CuO(290)
1073	CuO(45) $CuAl_2O_4$(184)	CuO(258) $CuAl_2O_4$(198)	CuO(332) $CuAl_2O_4$(210)	CuO(350) $CuAl_2O_4$(244)
1273	CuO(60) $CuAl_2O_4$(513)	CuO(478) $CuAl_2O_4$(532)	CuO(468) $CuAl_2O_4$(491)	CuO(552) $CuAl_2O_4$(484)

[a] HT= copper aluminum carbonate hydroxide hydrate; Ma = malachite; Gi = gibbsite; Ge= gerhardtite

copper aluminate by a solid-state reaction. Larger copper oxide particles (see Table 3) could impede the diffusion of the ions and decrease the rate of formation of the spinel phase.[39−41]

The transition of the hydrotalcite layered structure to the mixed oxide structures, which takes place at temperatures lower than 500 K for all the samples, is completely reversible, even for calcination temperatures below 700 K. The layered structure is again recovered (around 25% for HT3.0 sample), if after this calcination process the samples are placed in an autoclave (for 2 days) in hot water at 353 K and CO_2 (total pressure = 10 atm). This reversible behavior also agrees with other results reported in the literature.[10,11,42,43]

FT-IR Spectroscopy. Figure 4 shows the FT-IR spectra of the noncalcined samples and those calcined at different temperatures from precursors HT0.5 and HT3.0.

The FT-IR spectra show a broad peak at 3300−3800 cm^{-1} for the samples calcined at lower temperatures. This broad peak is assigned to the stretching mode of hydrogen-bonded hydroxyl groups from the gibbsite and brucite-like layers and from the interlayer water molecules. The broader peak increases because it overlaps with a shoulder above 3000 cm^{-1}, which is assigned to ν_{OH} of water molecules hydrogen-bonded to carbonate ions in the interlamellar layer.[6,7,33,34,44−46] Consequently, this band is much broader when the samples contain a higher amount of carbonate. It seems that the carbonate content increases when the Cu/Al atomic ratio in the sample is higher (HT1.0, HT2.0, and HT3.0) than when it is not (HT0.5), in agreement with the chemical analysis (see Table 1). Also, the position of this band shifts to the region of higher frequency when there is more aluminum in the sample.

Furthermore, the water deformation band is recorded around 1600 cm^{-1}, which overlaps with a double band that appears about 1350−1500 cm^{-1} for samples HT1.0, HT2.0, and HT3.0 but not for the HT0.5 sample, when they are calcined at lower temperatures. This double band could be assigned to the carbonate and nitrate anions in the interlayer of the hydrotalcite-like compounds[24] and probably to the carbonate anions resulting from the traces of malachite phase detected in the samples HT2.0 and HT3.0.

On the other hand, only a weak peak is detected around 1350−1390 cm^{-1} for HT0.5 (which has the highest amount of nitrate anions). This is also probably due to the nitrate and carbonate anions.[47]

It is well-known that the carbonate anion in a symmetric environment is characterized by a D_{3h} planar symmetry. The three IR active absorption bands observed from the carbonate anion are detected at 1350−1380 cm^{-1}, 850−880 cm^{-1}, and 670−690 cm^{-1}.

Also, the ν_3 vibration of the nitrate anion is detected around 1376 cm^{-1}.[47]

However, the double band detected at 1350−1500 cm^{-1} may be attributed either to a lowering of the symmetry of the carbonate and nitrate anions from D_{3h} to C_{2v} in the interlayer or to the disordered nature of the interlayer.[34,35]

When the Cu/Al atomic ratios in the samples increase (in parallel with the increase of hydrotalcite phase), the intensity of this double band increases. These samples also have more carbonate anions (see Table 1). It has also been observed that this double band becomes much weaker when the calcination temperature increases.

Calcination temperatures higher than 800 K are required to remove this double band from the samples which have a higher copper content.

Furthermore, the peak around 1500 cm^{-1} is more stable at a higher temperature than the peak around 1380 cm^{-1}. We can conclude, therefore, that the rise in the Cu/Al atomic ratio increases the amount of carbonate anions in the interlayer and leads to different types of carbonate sites which have different interactions in the brucite-like layer.

Thermal Analysis. The TG diagrams for the four uncalcined samples are shown in Figure 5.

There was a considerable weight loss (≈40%) between 400 and 600 K during the thermal decomposition of the HT0.5 sample, and a small loss (≈2%) was detected at about 730 K. The weight loss between 400 and 600 K was also recorded for the other samples, but they always showed lower weight losses (≈25−33%). Furthermore, new weight losses were detected at higher decomposition temperatures when the copper contents in the sample increased (HT1.0, HT2.0, and HT3.0). This agrees with the data in the literature.[48] For example, sample HT1.0 shows two new weight losses between 850 and 1050 K which are observed at 650 and 900 K for the sample HT2.0 and at 840 K for the sample HT3.0. The changes in weight found for these samples at higher

(39) Shaikhutdinov, s. K.; Avdeeva, L. B.; Goncharova, O. V.; Kochubey, D. I.; Novgorodov, B. N.; Plyasova, L. M. *Appl. Catal.* **1995**, *126*, 125.
(40) Alzamora, L. E.; Ross, J. R. H.; Druissink, E. C.; van Rejen, L. L. *J. Chem. Soc., Faraday Trans.* **1981**, 1, *77*, 665.
(41) Zielinski, J. *Appl. Catal. A* **1993**, *94*, 107.
(42) Rey, F.; Fornés, V.; Rojo, J. M. *J. Chem. Soc., Faraday Trans* **1992**, *88*, 2233.
(43) Constantino, V. R. L.; Pinnavaia, T. J. *Inorg. Chem.* **1995**, *34*, 883
(44) Kooli, F.; Rives, V.; Ulibarri, M. A. *Inorg. Chem.* **1995**, *34*, 5122.
(45) Cavani, F.; Clause, O.; Trifiró, F.; Vaccari, A. *Adv. Catal. Des.* **1991**, 186.
(46) Kruissink, E. C.; Van Reijden, L. L.; Ross, J. R. H. *J. Chem. Soc., Faraday Trans. 1* **1981**, *77*, 649.
(47) Velu, S., Ramkumar, V.; Narayanan, A.; Swamy, C. S. *J. Mater. Sci.* **1997**, *32*, 957.
(48) Velu, S.; Swamy, C. S. *J. Mater. Sci. Lett.* **1996**, *15*, 1674.

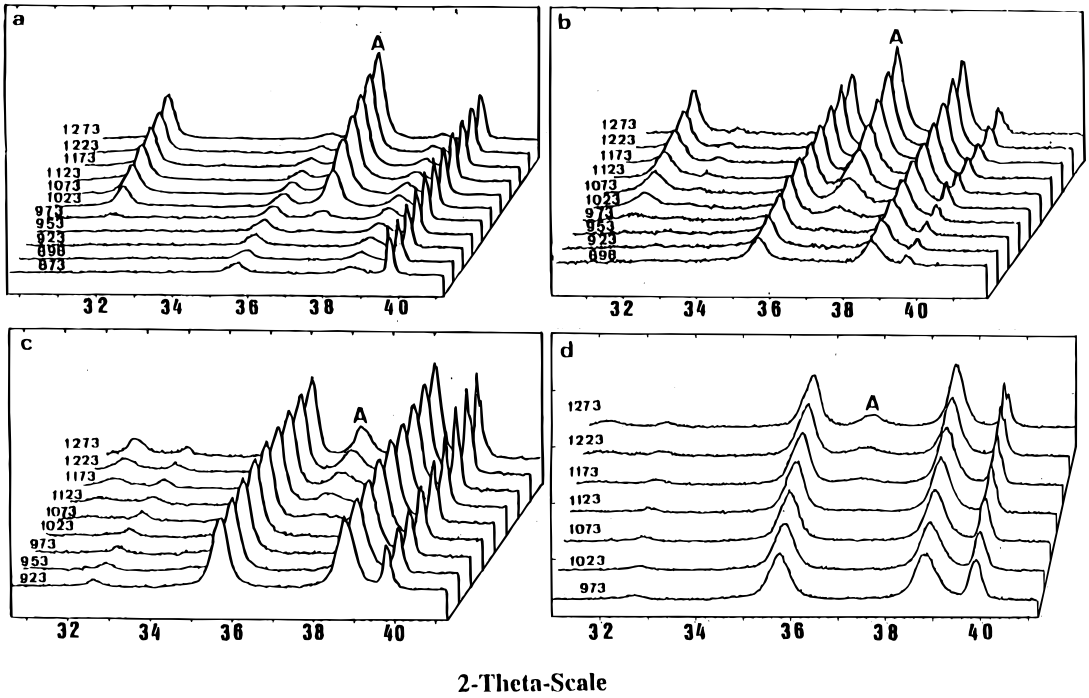

Figure 3. Evolution of the X-ray diffractograms versus calcination temperatures between 873K and 1273K of the (a) HT0.5, (b) HT1.0, (c) HT2.0, and (d) HT3.0 samples performed in situ with a high-temperature XRD attachment. Letter A indicates the *hkl* (311) diffraction line of the copper aluminate.

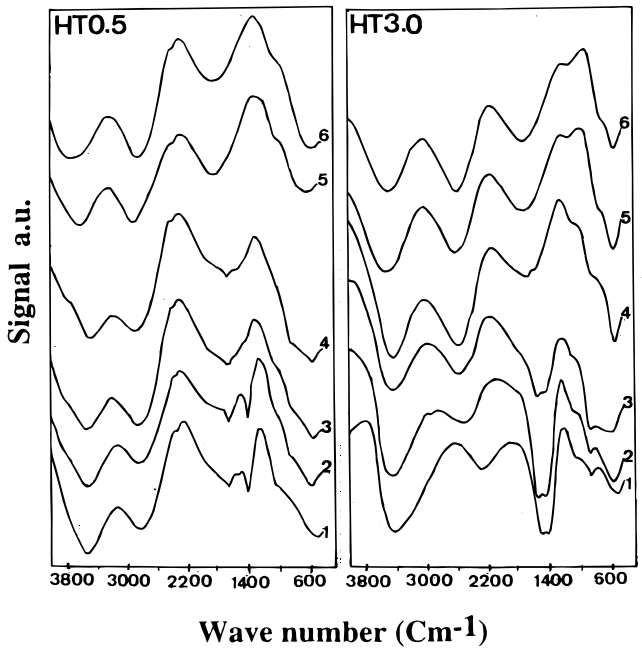

Figure 4. IR spectra of samples HT0.5 and HT3.0 calcined at different temperatures: (1) 333 K; (2) 473 K; (3) 673 K; (4) 873 K; (5) 1073 K, and (6) 1273 K.

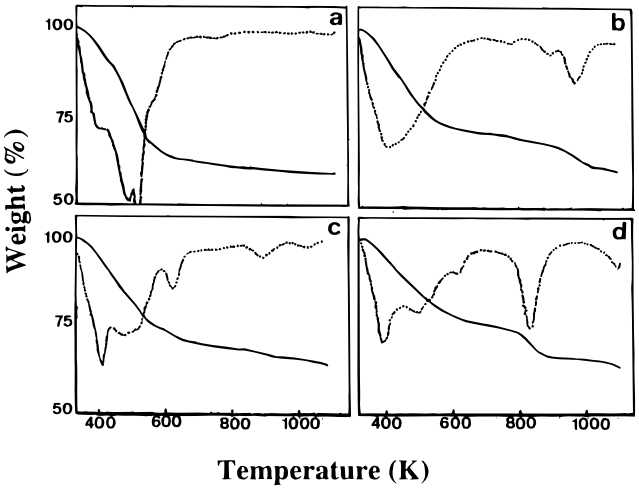

Figure 5. Weight decrease versus temperature for the thermal decomposition of samples (a) HT0.5, (b) HT1.0, (c) HT2.0, and (d) HT3.0.

temperatures are between 8% and 12%, and the total weight loss (from room temperature to 1173 K) was around 40% for the four samples. A decrease of total weight loss (<5%) is observed when the copper content increases.

The nature of the gases released during the thermal treatment was monitored by mass spectrometry detecting the masses 18, 17 (H_2O); 30, 14 (NO); 30, 46 (NO_2) and 44, 28 (CO_2).

Plots of the MS data as a function of temperature, for the HT.05, HT1.0, HT2.0, and HT3.0 noncalcined samples and a pure malachite phase as reference, are given in Figure 6,parts a, b, c, d, and e, respectively.

The main species detected by mass spectrometry during the decomposition process are H_2O and CO_2 for the pure malachite phase (e) and H_2O, CO_2, NO_2, and NO for the HT0.5, HT1.0, HT2.0, and HT3.0 samples. These samples have a carbonate/nitrate ratio of 2.4, 3.1, 6.4, and 11.0, respectively (see Table 1). So, when the copper contents increase, there is more carbonate in the sample.

A broad band of water is detected between 400 and 800 K for the samples (see Figure 6a−d). The first main peak in water loss, at lower temperature (380−500 K), is mainly due to the removal of weakly bonded water, which is probably the hydration water located in the interlayer space of the copper hydrotalcite phase. This

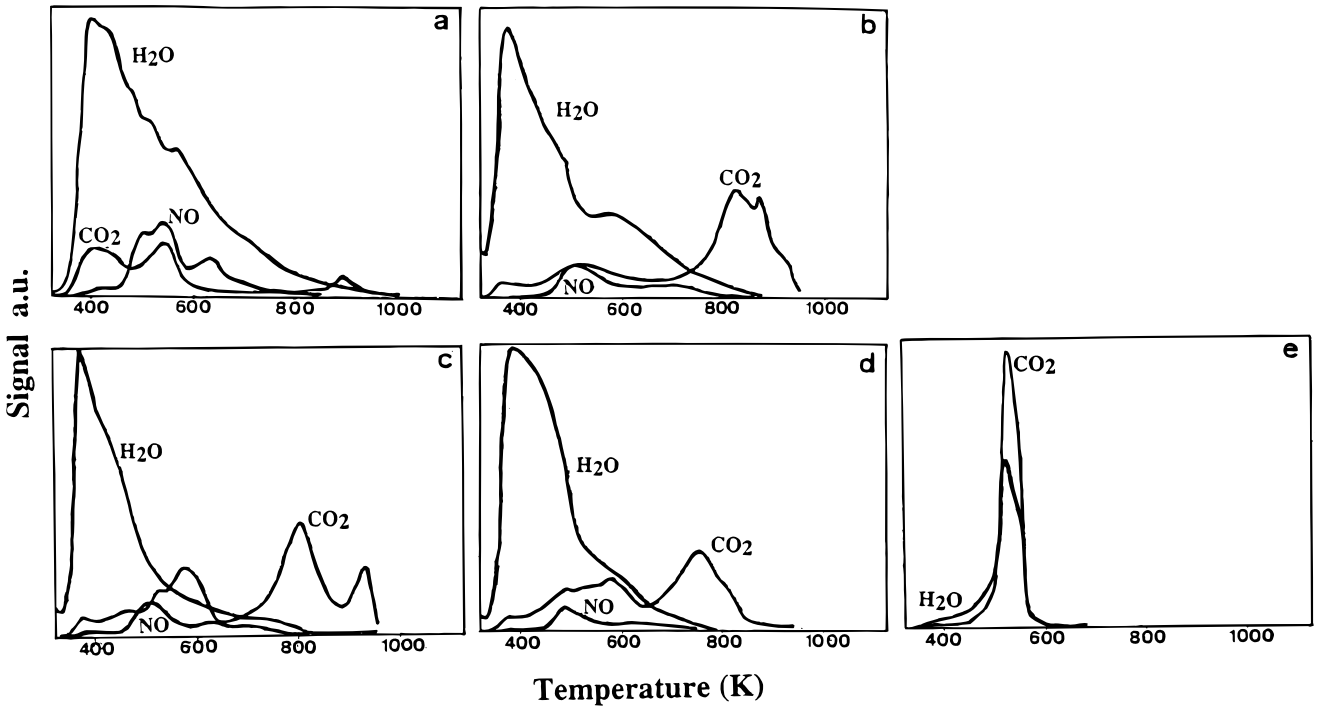

Figure 6. Thermal decomposition versus temperature performed in an ultrahigh vacuum mass spectrometer for the samples (a) HT0.5, (b) HT1.0, (c) HT2.0, (d) HT3.0, and (e) a malachite sample as reference.

process is accompanied by the removal of traces of gases such as CO_2, NO_2, and NO. These gases are probably produced by the decomposition of carbonate and nitrate anions, located at the end of the interlayer space, that are weakly bonded.[12]

Furthermore, a second loss of water, which always overlapped with the first loss of water, has been detected between 500 and 700 K, depending on the copper content of the sample. This second water loss is also accompanied by the removal of NO, NO_2, and CO_2. The CO_2, NO_2, and NO gases are evolved when the carbonate and nitrate anions from the interlayer decompose, and the water is produced when the hydroxyl groups condense in the brucite-like layer.

The loss of water detected at higher temperatures (>700 K) for the sample HT0.5 can probably be assigned to the condensation process of the hydroxyl groups in the alumina phase (gibbsite). It is important to note that much less NO_2 was detected during the decomposition processes than NO. This is probably due to experimental conditions (vacuum and free air atmosphere).

There were new CO_2 emissions from samples with higher Cu/Al atomic ratios (HT1.0 to HT3.0) between 700 and 1000 K, and this agrees with the data in the literature.[48] These new CO_2 emissions are probably due to the fact that the carbonate anion, which interacts strongly in the brucite-like layer, decomposes. The evolution of these gases causes the hydrotalcite-type structure to decompose totally, and this initial structure cannot then be recovered under hydrothermal treatments.

On the other hand, only one narrow band (500−580 K) of water and CO_2 emissions was obtained during the decomposition process of the pure malachite sample.

The emission of CO_2 at higher temperature observed for the copper hydrotalcite-like phase is explained by the fact that, during the thermal decomposition of the samples, there is some type of reaction with the carbonate anions in the interlayer space to form some sort of "oxycarbonates".[48] However, this fact cannot explain the peak detected by FT-IR around 1500 cm^{-1} at room or lower calcination temperatures for the samples with higher Cu/Al atomic ratios.

The CO_2 emission processes of the samples could probably be better explained by two different types of carbonate coordinations in the brucite-like layer. The carbonate anion can behave as a monodentate or bidentate ligand in the interlayer region.[49,50] The monodentate carbonate decomposes at a lower temperature, whereas the bidentate carbonate is more stable at higher temperatures. This mechanism can explain the splitting of the bands detected by FT-IR about 1350−1500 cm^{-1} for the samples with higher copper contents.

We suggest therefore that this bidentate carbonate, which decomposes at temperatures higher than 700 K, is probably responsible for the peak detected by FT-IR around 1500 cm^{-1}.

Temperature Programmed Reduction (TPR). The TPR profiles of the noncalcined CuAl−HT samples are given in Figure 7. The composition of the evolved gases was monitored with a quadrupole mass spectrometer. The reduction process (H_2/Ar, 5/95 vol) was studied to check whether any compensating anions were reduced together with the Cu^{2+} ions during the TPR experiment. Masses such as H_2 (2), NO_2 (30, 46), NO (14, 30), N_2O (14, 28, 44), NH_3 (17), H_2O (17, 18), CO_2 (44, 28), and CO (28) were particularly monitored, taking into account the nature of the exchangeable anions in the interlayer space, such as carbonate and nitrate. Water, CO_2, and NO were the main species detected.

(49) Miyata, S. *Clays Clay Miner.* **1975**, *23*, 369.
(50) Miyata, S.; Okada, A. *Clays Clay Miner.***1977**, *25*, 14.

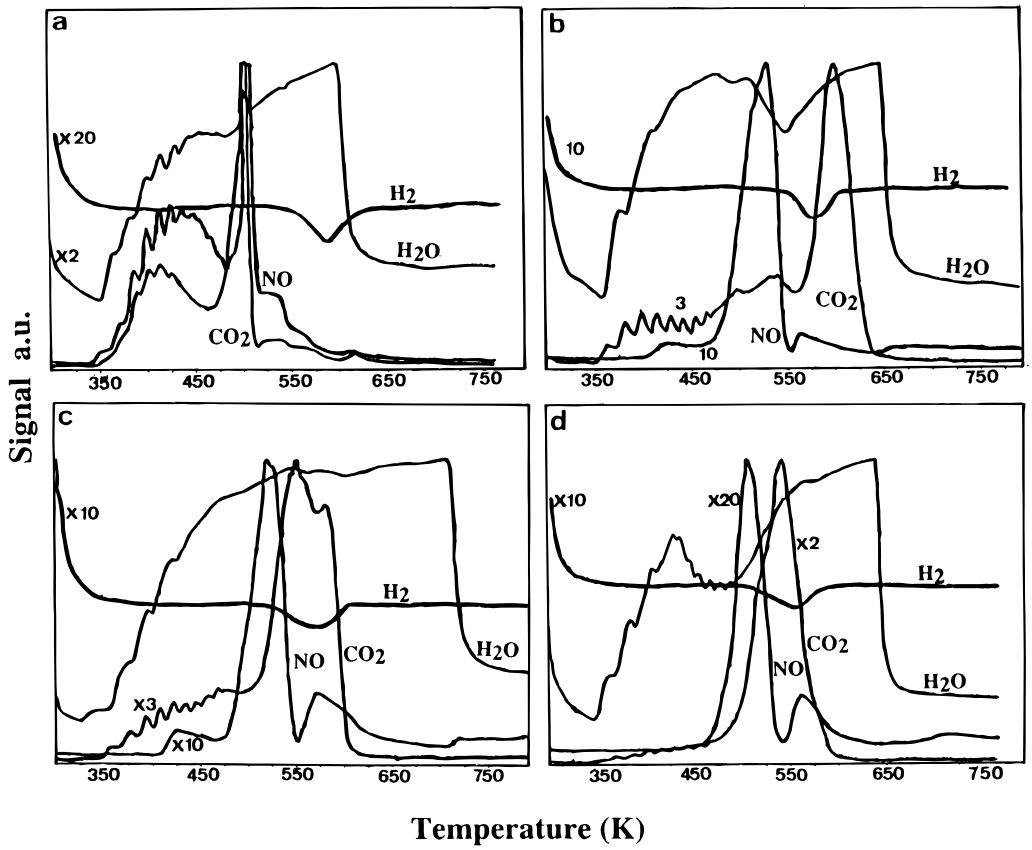

Figure 7. Temperature-programmed reduction followed by mass spectrometry of the noncalcined (a) HT0.5, (b) HT1.0, (c) HT2.0, and (d) HT3.0 samples.

The water evolution profiles for the four samples show a broad band between 350 and 700 K. These results are similar to the ones obtained during the decomposition process. Likewise, the evolution of the NO from the nitrate anion has a similar trend for both the decomposition and the reduction processes. There was a main NO peak around 500 K during the TPR experiments. This peak is also accompanied by a shoulder at around 580 K for HT1.0, HT2.0, and HT3.0 samples. However, CO_2 did not behave in the same way as far as the decomposition and the reduction processes are concerned. There was a considerable decrease in the temperature of CO_2 evolution during the TPR experiment compared with the decomposition process in the absence of hydrogen. The total release during the TPR experiment takes place at temperatures lower than 650 K instead of around 700−1000 K for the decomposition process. It can be stated that the hydrogen atmosphere favors the carbonate decomposition process.

It is important to mention that CO_2 is always released at higher temperatures than the NO for the three samples that have the highest Cu/Al atomic ratios. In contrast, for the HT0.5 sample, CO_2 and NO are evolved at the same temperature and around 500 K.

Moreover, the reduction process of the Cu^{2+} in the samples starts when practically all the nitrate anions have been decomposed.

On the other hand, for the samples with the highest Cu/Al atomic ratios, the Cu^{2+} is reduced to Cu at the same time as the CO_2 is released. It seems that for these samples the reduction of the Cu^{2+} to Cu may be related to the decomposition or incipient reduction of the carbonate ions.

As previously discussed in the thermal analysis and FT-IR section, the presence of two types of carbonate coordination in the brucite-like layer has been mentioned. The bidentate carbonate is probably strongly bound to the Cu^{2+} of the layers, while the monodentate carbonate is loosely bound in the interlayer region.

The CO_2 released during the reduction of the copper ions (about 500−600K) for the HT1.0, HT2.0, and HT3.0 samples probably comes from the same bidentate carbonate that, in the absence of hydrogen, would have decomposed at higher temperature (see Figure 6). This may be explained assuming that the Cu^{2+}−carbonate bidentate bond must cleave with the reduction of Cu^{2+} to metallic copper.

However, the carbonate decomposition to CO_2 does not consume hydrogen, since the amount consumed is always very close to that required for the stoichiometric reduction of Cu^{2+} to Cu. We may conclude that the CO_2 release is favored by the presence of reduced copper. So, it can be stressed that decomposition of the hydrotalcite-like phase takes place in the same temperature range as the reduction of copper ions.

In contrast, for the HT0.5 sample, the reduction of the Cu^{2+} to Cu takes place about 100 K higher than the carbonate and nitrate decomposition processes.

The reduction process of the Cu^{2+} happens at temperatures between 500 and 650 K for the four samples. Furthermore, when the Cu/Al atomic ratios of the samples decrease, there is an increase in the reduction temperature because there is greater interaction between the Cu^{2+} and the alumina.

Some TPR experiments were also performed using the TG conditions for the samples HT0.5 and HT3.0 calcined

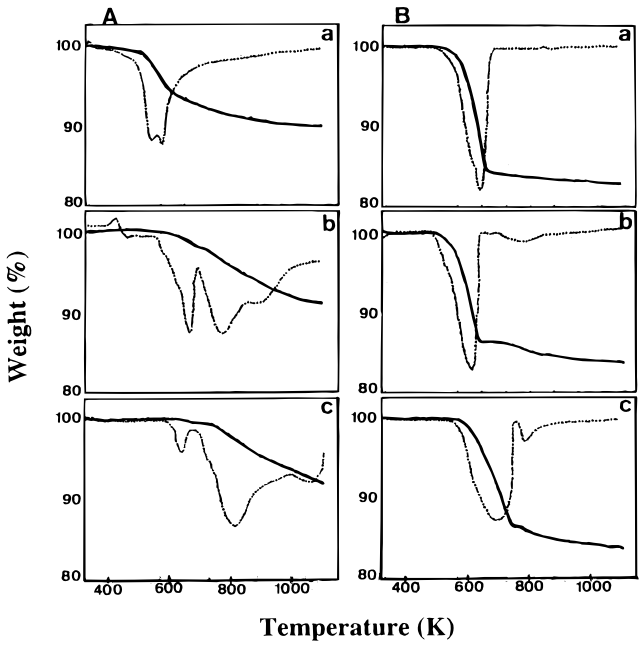

Figure 8. Temperature-programmed reduction profiles of the (A) HT0.5 and (B) HT3.0 samples calcined at (a) 873 K, (b) 1073 K, and (c) 1273 K.

(with a heating rate of 1 K/min and maintaining the final temperature for 16 h) at higher temperatures (873, 1073, and 1273 K) (see Figure 8). At these calcination temperatures, the nitrate and practically all the carbonate anions are decomposed. The samples calcined at 873 K (a) show an initial reduction temperature that is shifted to higher temperatures with the increase in copper content. This effect can be explained if we take into account the higher dispersion of the oxide phase (CuO) in the sample HT0.5, which supplies the reduction process.[41]

On the other hand, the reduction process is longer for HT0.5 than for HT3.0. This fact can be explained in terms of a strong interaction between the small CuO particles (detected in HT0.5) and the alumina surface, forming a nonstoichiometric copper aluminate phase onto the alumina surface that is reduced at higher temperatures.[37,51−53] Furthermore, the degree of reduction for the samples calcined at lower temperatures (<873 K), which was calculated by measuring the weight loss during the reduction process, is practically 100%. This reduction process is mainly assigned to the reduction process of the copper oxide. Moreover, new peaks were detected when the calcination temperature increased. These peaks shift to higher temperatures when the calcination temperature increases and when the Cu/Al ratio values decrease. For example, the reduction process shifts at a higher temperature when the calcination temperature increases for sample HT0.5 (see Figure 8A). In contrast, the increase in the calcination temperature does not greatly influence the reduction process for the sample HT3.0 (see Figure 8B).

The reduction process is therefore strongly affected by the low copper contents and high calcination temperatures. These effects cause a decrease in the degree

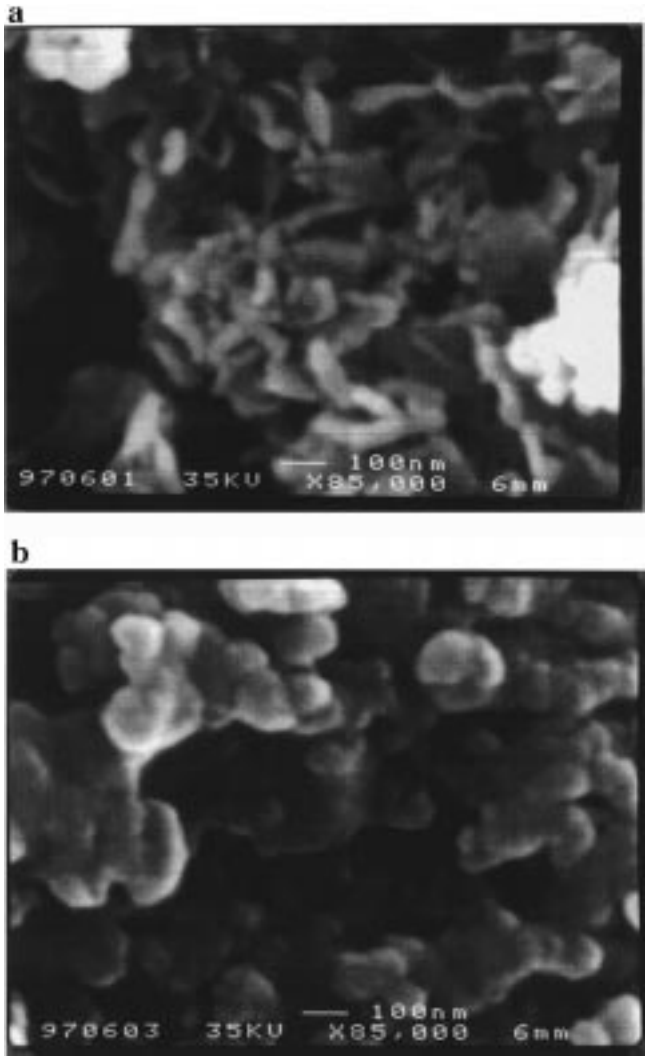

Figure 9. Scanning electron micrographs from the (a) noncalcined sample HT3.0 and (b) the sample calcined at 1273 K.

of reduction of the samples. For example, the HT0.5 samples calcined at 1073 and 1273 K and reduced up to 1173 K (see Experimental Section) show a reduction degree of 90% and 80%, respectively, instead of the 97% and 95% achieved by the HT3.0 samples at the same calcination temperatures. This is explained in terms of the copper aluminate spinel phase that is formed by the interaction of the copper oxide with the alumina.[51−53] This phase has also been detected by XRD. Furthermore, the TPR shows that over 99% of copper oxide turns into copper aluminate in sample HT0.5(1273), whereas only 15% of the copper oxide turns into copper aluminate in sample HT3.0(1273).

Electron Microscopy (SEM). A stereographic picture of the noncalcined HT3.0 sample is shown in Figure 9a. All noncalcined samples show similar stereographic pictures. The morphologies of these samples are characteristic of hydrotalcite-like materials,[54−56] with a platelet thickness ranging from 15 to 25 nm. The

(51) Lo Jocano, M.; Cimino, A.; Inversi, M. *J. Catal.* **1982**, *76*, 320−332.
(52) Susnitxky, D. W.; Carter, C. B. *J. Mater. Res.* **1991**, *6*, 1958.
(53) Ciampi, S.; Di Castro, V. *Surf. Interface Anal.* **1994**, *22*, 594.
(54) Szymanski, R.; Travers, C.; Chaumette, P.; Courty, P.; Durand, D. In *Preparation of Catalysts IV*; Delmon, B., Jacobs, P. A., Poncelt, G., Eds.; Elsevier: Amsterdam, 1987; p 738.
(55) Thevenot, F.; Szymanski, F.; Chaumette, P. *Clays Clay Miner.* **1989**, *37*, 396.
(56) Medina, F.; Dutartre, R.; Tichit, D.; Coq, B.; Dung, N. T.; Salagre, P.; Sueiras, J. E. *J. Mol. Catal.* **1997**, *119*, 201.

platelet thickness increases with the Cu content. The sheet morphologies are also more crystalline when the copper content is higher. Calcination temperatures, even lower than 550 K, can destroy the sheet structure. This structure is more stable for the samples with higher Cu/Al atomic ratios. This behavior is also revealed by XRD. A nodular appearance is observed after calcination up to 673 K. These nodules of about 4−13 nm are the CuO particles also detected by XRD. The particle size of the CuO phase increases when both the calcination temperature and the amount of copper increase. Furthermore, when the calcination temperature is raised to 1073 K, a strong structural change takes place in the morphology of the samples. This effect causes a loss of porous structure and the formation of a copper aluminate phase which undergoes a considerable sinterization when the calcination temperature rises to 1273 K (see Figure 9b).

Conclusions

Copper−aluminum samples with Cu/Al atomic ratios between 0.5 and 3.0 were prepared using trimethylamine and CO_2 as precipitants. Several techniques such as TG, XRD, BET areas, FT-IR, SEM, and TPR were performed to characterize the solids obtained. The thermal stability, crystallinity, and purity of the materials depended on the Cu/Al atomic ratio added during the coprecipitation process.

The copper hydrotalcite phase was sometimes accompanied by other phases such as gibbsite, malachite, and gerhadtite. The copper hydrotalcite phase was stable and more pure at high Cu/Al atomic ratios. The FT-IR and TG detected carbonate (mainly) and nitrate as counteranions which show different interactions in the interlayer region. There are both loosely bound carbonate and nitrate anions and a strongly bound carbonate that decomposes at higher temperatures. The evolution of the phases obtained during the calcination process was studied by dynamic XRD experiments.

The copper hydrotalcite phase is only stable at calcination temperatures lower than 500 K. All the samples showed a well-dispersed CuO (at low calcination temperatures) and copper aluminate phase (at higher calcination temperatures). The particle sizes obtained for the CuO and $CuAl_2O_4$ phases had values between 4 and 55, and 18 and 53 nm, respectively.

A pure copper aluminate of high surface area (>150 m^2/g) can also be obtained from the calcination of the HT0.5 sample.

The rate of formation of copper aluminate considerably decreased when the amount of copper in the sample increased.

The materials obtained were also studied by TPR experiments. The carbonate anions decompose at much lower temperatures during the reduction process compared to the decomposition process in the absence of hydrogen. The consumption of hydrogen was always very close to that required for the stoichiometric reduction of Cu^{2+} to Cu, which suggests that the carbonate and the nitrate anions only undergo a decomposition process under the TPR conditions tested.

The degree of reduction of the samples calcined at higher temperatures decreases both when the calcination temperature increases and the copper content decreases, i.e., the reduction degree for the samples HT0.5(1073) and HT0.5(1273) were 90% and 80%, respectively, as opposed to 97% and 95% for the sample HT3.0 at the same calcination temperatures. These effects can be explained by the formation of a spinel phase such as copper aluminate produced by the interaction of the copper oxide with the alumina.

In conlusion, we have found that higher dispersions for both the CuO and the copper aluminate phases can be obtained from calcination of copper−aluminum samples at different temperatures. The dispersion is higher when the Cu/Al atomic ratio of the sample decreases. For example a pure copper aluminate of high surface area (>150 m^2/g) can be obtained from the calcination of the HT0.5 sample, and this fact is of potential interest in oxidation reactions.[28,29]

CM980500F